Well-defined diblock brush polymer-drug conjugates for sustained delivery of paclitaxel

Journal:	*Biomaterials Science*
Manuscript ID:	BM-ART-12-2014-000458.R1
Article Type:	Paper
Date Submitted by the Author:	29-Jan-2015

Complete List of Authors:	Zou, Jiong; Univeristy at Buffalo, the State University of New York, Department of Chemical and Biological Engineering Yu, Yun; Univeristy at Buffalo, the State University of New York, Department of Chemical and Biological Engineering Li, Yukun; Univeristy at Buffalo, the State University of New York, Department of Chemical and Biological Engineering Ji, Wei; Univeristy at Buffalo, the State University of New York, Institute for Lasers, Photonics and Biophotonics, and Department of Chemistry Chen, Chih-Kuang; Univeristy at Buffalo, the State University of New York, Department of Chemical and Biological Engineering Law, Wing-Cheung; Univeristy at Buffalo, the State University of New York, Institute for Lasers, Photonics and Biophotonics, and Department of Chemistry Prasad, Paras; Univeristy at Buffalo, the State University of New York, Institute for Lasers, Photonics and Biophotonics, and Department of Chemistry Cheng, Chong; Univeristy at Buffalo, the State University of New York, Department of Chemical and Biological Engineering

Cite this: DOI: 10.1039/c0xx00000x

www.rsc.org/xxxxxx

ARTICLE TYPE

Well-defined diblock brush polymer-drug conjugates for sustained delivery of paclitaxel†

Jiong Zou,[a] Yun Yu,[a] Yukun Li,[a] Wei Ji,‡[b] Chih-Kuang Chen,[a] Wing-Cheung Law,[b] Paras N. Prasad,[b] and Chong Cheng*[a]

Received (in XXX, XXX) Xth XXXXXXXXX 20XX, Accepted Xth XXXXXXXXX 20XX
DOI: 10.1039/b000000x

Using the 3rd generation of Grubbs' catalyst as the initiator, diblock brush polymer drug conjugates (BPDCs) were synthesized by sequential ring-opening metathesis polymerization (ROMP) of a hydrophilic poly(ethylene glycol) (PEG)-based norbornene (NB)-functionalized macromonomer and a hydrophobic paclitaxel (PTXL)-based NB-functionalized monomer. These amphiphilic diblock BPDCs had well-defined structures, with narrow molecular weight distributions (M_w/M_n = 1.10-1.16). They self-assembled into multi-molecular nanostructures in aqueous solutions. Although the PTXL moieties were connected to backbone with cycloacetal-based conjugation linkages, the cleavage of these linkages from the assemblies of diblock BPDCs was relatively slow and exhibited limited acid-sensitivity, indicating significant influence of the macromolecular structure and assembly of BPDCs on their drug release behaviour. Cytotoxicity study not only showed that the diblock BPDCs were therapeutically effective against cancer cells, but also revealed a correlation between cytotoxicity and grafting structures of BPDCs. In summary, the results obtained in this work provide new insights towards the structure-dependent properties of brush polymer-based drug delivery systems.

Introduction

With versatile properties, polymers have been broadly investigated for applications in drug delivery.[1-5] Drugs can be loaded into polymers by either encapsulation or conjugation. For drug-encapsulated systems, the drug is physically trapped in polymer matrix and its release is realized through diffusion. Therefore, their drug release behaviour can be effectively tuned through the matrix properties. For instance, because the diffusion resistance for encapsulated drug molecules decreases with the dissociation of assembled scaffolds, drug release can be manipulated through the triggered disassembly of scaffolds.[6] On the other hand, drug release from polymer-drug conjugates (PDCs) is more complicated, because the cleavage of the conjugation bond is required before the drug moieties can diffuse from the polymeric scaffolds.[7-8] In principle, the drug release behaviour of PDCs can be affected by the structures and properties of not only the conjugation bonds, but also the entire scaffolds.

Because cancer is a leading cause of death, the delivery of anticancer drugs, such as paclitaxel (PTXL), doxorubicin (DOX) and camptothecin (CPT), using polymer-based systems has attracted broad interest.[9-15] Comprehensive considerations are required to design polymeric scaffolds for anticancer drug delivery.[1,13] Specifically, it is important to control the dimensions of these scaffolds within the range of 10-200 nm, in order to avoid rapid clearance and to enable passive tumour targeting via the enhanced permeability and retention (EPR) effect.[16]

With densely grafted macromolecular architectures, brush polymers can possess a variety of well-defined unimolecular nanostructures, as well as intermolecularly assembled superstructures.[17-21] Drug delivery using brush polymers as encapsulation scaffolds has attracted considerable interests in recent year.[22-29] Brush copolymers with amphiphilic poly(ε-caprolactone)-*b*-poly(ethylene glycol) (PCL-*b*-PEG) diblock grafts have been studied for the encapsulation and release of doxorubicin (DOX).[22-23] As reported by Wang and co-workers,[22] these brush copolymers assembled into spherical multi-molecular micelles in aqueous solutions, and these micelles exhibited higher loading and slower release of DOX than the spherical micelles of the corresponding linear PCL_{19}-*b*-PEG_{45} diblock copolymer. Similar systems with longer PEG blocks were studied by Chen and co-workers;[23] however, unimolecular micelles were obtained from these brush copolymers, and they showed lower loading and faster release of DOX than the spherical micelles of the corresponding linear PCL_{17}-*b*-PEG_{113} diblock copolymer. Comparison of the results reported by these two groups indicated that the assembly behaviour of brush polymers can critically affect their drug encapsulation and release performance. Brush copolymers with block structures have also been investigated for drug delivery applications. For instance, amphiphilic diblock brush copolymers having a cholesterol-containing block and a PEG-based block were studied by Kasi, Lu and co-workers.[24-25] The self-assembled nanostructures of these copolymers were capable of encapsulating a high wt% of DOX, and in vivo studies showed that the resulting DOX-loaded nanostructures can lead to improved DOX delivery to tumour tissues as compared to free DOX.[25]

Recently, brush polymer-drug conjugates (BPDCs) have also been synthesized and studied.[30-36] Based on ring-opening metathesis polymerization (ROMP), Johnson et al. obtained BPDCs with each backbone repeat unit simultaneously carrying a PEG chain and a photocleavable drug (DOX or CPT) moiety.[30-31]

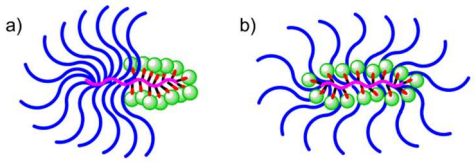

Fig 1 Schematic illustrations of a) diblock BPDC, and b) statistical BPDC.

We also prepared BPDCs by statistical copolymerization of a PEG-based norbornene (NB)-functionalized macromonomer and PTXL-based NB monomer with an acid-sensitive cycloacetal-based conjugation linkage.[32] In each case, the light scattering data suggested the presence of unimolecular micelles of BPDCs in aqueous solutions, and environmentally triggered cleavage of conjugation linkage for drug release was observed.[30-32]

Based on our previous work on the BPDCs as statistical copolymers,[32] we are interested in investigating BPDCs with block-wise distribution of pendent drug moieties and hydrophilic grafts, in order to further evaluate the influence of the structures of BPDCs on their assembly behaviour, drug release profile and therapeutic effects. To the best of our knowledge, such diblock BPDCs have not been reported. In this article, we report the first examples of well-defined diblock BPDCs. Results on the synthesis, characterization and property studies of the diblock BPDCs are described. Comparisons of the properties of the diblock BPDCs and the statistical BPDCs (Fig. 1) are further made to reveal the correlations between the structures and properties of BPDCs, and to provide insightful guidance on the structural design of BPDCs for achieving optimal drug delivery behaviour.

Experimental

Measurements

^{1}H NMR spectra were obtained on a Varian INOVA-500 spectrometer at room temperature. The samples were dissolved in $CDCl_3$ containing 1.0 vol% tetramethylsilane (TMS) as an internal reference.

Gel permeation chromatography (GPC) was conducted using Viscotek GPC system equipped with a VE-3580 refractive index (RI) detector, a 270 dual detector system having a viscometer detector and a dual-angle (7º and 90º) laser light scattering detector, a VE 1122 pump, and two mixed-bed organic columns (PAS-103M and PAS-105M). *N*,*N*'-dimethylformamide (DMF; HPLC grade) with 0.1 M LiBr was used as solvent for polymers and eluent for GPC with a flow rate of 0.50 mL/min at 55 ºC. Polymer solutions were prepared at a known concentration (ca. 2.0 mg/mL) and an injection volume of 100 µL was used. The system was calibrated with linear polystyrene standards with narrow polydispersities (PDI < 1.1; Polymer Laboratories, Varian Inc.).

HPLC analysis was performed on Agilent 1100 series HPLC system with G1322A online degasser, G1312A binary pump, and G1313A autosampler. Chromatographic separation was achieved by using a reversed phase C18-column (ZORBAX SB-C18, 250 × 4.6 mm, 5 µm) at 25 ºC. The mobile phase consisted of deionized water and HPLC grade acetonitrile, with linear gradients of acetonitrile/water (1:9~4:6 v/v, 0~10 min; 4:6~6:4 v/v, 10~15 min; 6:4~4:6 v/v, 15~22 min; 4:6~1:9 v/v, 22~24 min) at a flow rate of 1.0 mL/min. The UV wavelength for the detection of PTXL-based moieties was set at 227 nm.[37]

Dynamic light scattering (DLS) measurements were performed using a Nano ZS90 Zetasizer (Malvern Instruments). A 4 mW 633 nm HeNe laser was used as the light source and all experiments were performed at room temperature with a measuring angle of 90º to the incident laser beam. The correlation decay functions were analyzed by cumulants method coupled with the Mie theory to obtain size distribution.

Transmission electron microscopy (TEM) images were obtained by using a JEOL 2010 microscope. TEM samples were prepared by dip coating 300 mesh carbon-coated copper grids with dilute solutions of BPDCs (~0.2 mg/mL). A freshly prepared 0.2 % solution of ruthenium tetroxide (RuO_4) obtained by the reaction between sodium periodate and hydrated ruthenium dioxide in water was used as the staining agent for the TEM samples.[38] The dried samples were treated with the volatile vapour of RuO_4 prior to TEM measurements.

Materials

The 1st generation Grubbs catalyst, benzylidenebis(tricyclohexylphosphine)dichlororuthenium, was purchased from Sigma-Aldrich. Ethyl vinyl ether (EVE; 99%) was purchased from Acros. Dichloromethane (DCM; HPLC) was purchased from Fisher Chemical, and dried by distillation over CaH_2. All chemicals were used without further purification unless stated otherwise. The 3rd generation Grubbs catalyst, dichloro[1,3-bis(2,4,6-trimethylphenyl)-2-midazolidinylidene](benzylidene)bis(3-bromopyridine)ruthenium(II), was prepared according to a literature method.[39] PEG-based NB macromonomer **1** and the PTXL-based NB macromonomer **2** were prepared following the synthetic approaches we reported previously.[32]

ROMP Synthesis

Diblock BPDCs were synthesized using the following procedure. To a 10 mL Schlenk flask with a magnetic stir bar were added PEG-based macromonomer **1** (101 mg, 0.042 mmol) and DCM (2.0 mL; as reaction solvent) under a nitrogen atmosphere. After **1** was completely dissolved, a DCM solution of the 3rd Grubbs catalyst (1.48 mg, 1.26×10^{-3} mmol for the synthesis of BPDC **3a**; 0.37 mg, 4.2×10^{-4} mmol for the synthesis of BPDCs **3b** and **3c**) was added to induce polymerization at room temperature. When the polymerization time for the first block (15-60 min) was reached, a DCM solution of PTXL-based monomer **2** (50 mg, 0.042 mmol) was added, and then the polymerization solution was quenched 15-30 min later with ethyl vinyl ether. The polymerization solution was then precipitated in cold diethyl ether and gave BPDC as a white solid.

A BPDC **4** was prepared by statistical copolymerization of **1** and **2** initiated by the 3rd Grubbs catalyst ($[\mathbf{1}]_0$:$[\mathbf{2}]_0$:$[I]_0$ = 25:25:1), as we reported previously.[32] A PEG-based brush polymer **5** was prepared following the same procedure for the preparation of BPDC **4**, except that PTXL-based monomer **2** was not added to the polymerization system.

Drug Release Study

The pH 7.4 and pH 5.5 phosphate buffer solutions with 0.04 mg/mL of BPDC were prepared. At different time intervals,

every time 3 mL of BPDC solution was withdrawn and extracted by DCM (3 × 2 mL). Following our previously established procedure,[32] the extracted organic phase was separated by TLC, and the released PTXL-based moieties were collected and then quantified by HPLC analysis.

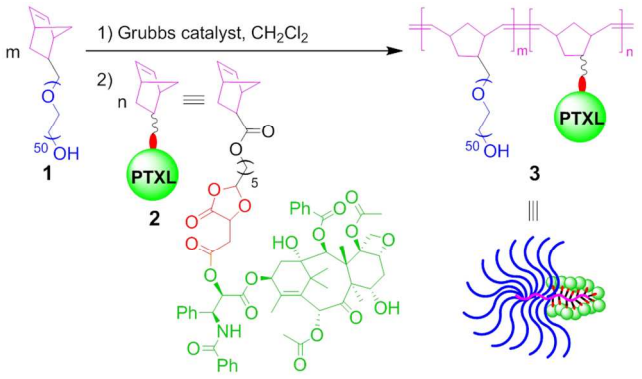

Fig. 2 Synthesis of diblock BPDCs **3** by sequential ROMP of PEG-based macromonomer **1** and PTXL-based monomer **2**.

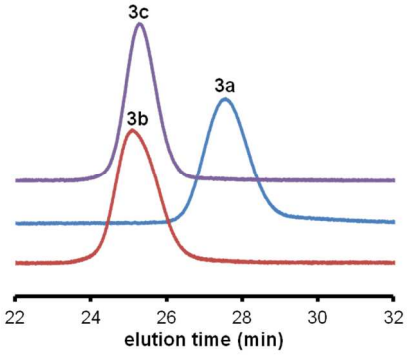

Fig. 3 GPC curves of BPDCs **3a**, **3b**, and **3c**.

Cytotoxicity Assay

The cytotoxicity of BPDC **3a** against cancer cells was assessed by the 3-(4,5-dimethylthiazol-2-yl)-5-(3-carboxymethoxyphenyl)-2-(4-sulfophenyl)-2H-tetrazolium (MTS) assay (Promega, Madision, WI). The cells were seeded onto a 96-well plate at a density of 5 × 10^3 to 1 × 10^4 cells per well in 180 μL of Dulbecco's modified Eagle's medium (DMEM) supplemented with 10% fetal bovine serum (FBS), and then 20 μL of samples with different BPDC concentrations were added. The cells were incubated for 48 h at 37 °C in 5% CO_2 atmosphere, followed by adding 110 μL of MTS solution. After incubating the cells for another 2 h, the resulting solutions were measured for absorbance at 490 nm by a multiwell plate reader (Opsys MR, Dynex). The cell viability was calculated as a percentage of absorbance of the sample well compared to that of the control well with untreated cells. The cytotoxicity of free PTXL, statistical BPDC **4**, and PEG-based brush polymer **5** as controls against cancer cells was evaluated with a similar procedure, except that trace amounts of DMSO (~0.1%, v/v) were present in the aqueous solutions of PTXL to increase its solubility.

Results and Discussion

With high reactivity and living characteristics, ROMP has been utilized for the synthesis of a variety of block brush polymers via "grafting through" different types of macromonomers.[40-41] Therefore, using the PEG-based NB-functionalized macromonomer **1** (M_n^{NMR} = 2.4 kDa, DP_{PEG}^{NMR} = 50, PDI^{GPC} = 1.1) and the PTXL-based NB macromonomer **2** (*MW* = 1188.27 Da), ROMP "grafting through" approach was selected for the synthesis of diblock BPDCs **3** in this work. The preparations of **1** and **2** were reported previously.[32] With a block-wise distribution of pendent PEG grafts and PTXL moieties, diblock BPDCs **3** were prepared by sequential polymerizations of **1** and **2** via ROMP in CH_2Cl_2 at room temperature (Fig. 2). Because the linear PEG chain of **1** is less bulky towards the NB group than the PTXL moiety of **2**, **1** was chosen as the first monomer for the ROMP process in order to get a fast crossover relative to the chain growth of the second block. Ru-based Grubbs' catalysts were selected as the initiators because of their high functional group tolerance. The 1st generation of Grubbs' catalyst was tried at first ($[\mathbf{1}]_0$:$[\mathbf{2}]_0$:$[I]_0$ = 25:25:1; 3 h for polymerization of **1**, 18 h for polymerization of **2**). However, GPC analysis of the resulting polymerization solution showed incomplete conversions of monomers, indicating insufficient reactivity of the catalyst. Therefore, the highly reactive 3rd generation of Grubbs' catalyst was synthesized and used as an initiator in ROMP ($[\mathbf{1}]_0$:$[\mathbf{2}]_0$:$[I]_0$ = 25:25:1 or 100:100:1) to yield well-defined poly(**1**)-*b*-poly(**2**) diblock BPDCs, i.e. **3a-c** (Table 1).[39] According to the GPC analysis of the polymerization solutions, the ROMP process was quite fast, leading to complete conversions of **1** and **2** within relatively short polymerization times. Their experimental M_n values determined by GPC were somewhat higher than the calculated values, presumably because of minor losses of the ROMP initiator at initiating stages.[42] The narrow molecular weight distributions of these diblock BPDCs (M_w/M_n = 1.06-1.16) further indicated the excellent living feature of the ROMP process (Fig. 3). ^{1}H NMR analysis verified the precise composition control in ROMP synthesis, and each of BPDCs **3a-c** had 50 mol% of **2** and 24 wt% of PTXL.[32] Based on the experimental M_n values of **3a-c**, it can be further estimated that on average each **3a** and **3b**/**3c** macromolecule carries ~35 and ~170 PTXL moieties, respectively.

Table 1. Preparation of diblock BPDCs by ROMP [a]

sample	$[\mathbf{1}]_0$:$[\mathbf{2}]_0$:$[I]_0$	Time [b] (h)	$M_{n,calcd.}$ [c] (kDa)	$M_{n,exptl.}$ [d] (kDa)	M_w/M_n [d]
3a	25:25:1	1 + 0.5	90	125	1.06
3b	100:100:1	1 + 0.5	360	594	1.16
3c	100:100:1	0.25 + 0.25	360	595	1.10

[a] Reaction conditions: dry DCM as solvent, room temperature; complete conversions of **1** and **2**. [b] Time = polymerization time of **1** + polymerization time of **2**. [c] $M_{n,calcd} = (M_{n,1} \times [\mathbf{1}]_0/[I]_0) + (MW_2 \times [\mathbf{2}]_0/[I]_0) + 104$. [d] By GPC with both RI and light scattering detectors.

Because the PEG-based poly(**1**) block is hydrophilic and the PTXL-based poly(**2**) block is hydrophobic, the diblock BPDCs **3** were expected to possess self-assembled nanostructures in aqueous solutions. Using **3a** and **3c** as the representative samples, the morphology of these diblock BPDCs were studied by using DLS and TEM. As determined by DLS in their aqueous solutions (Fig. 4), **3a** and **3c** showed Z-average hydrodynamic diameters (Z_{ave}) of 100.2 and 149.2 nm respectively, with a

mono-modal size distribution. Because the statistical BPDCs with the same composition and comparable M_n values exhibited much smaller hydrodynamic sizes,[32] it can be inferred that **3a** and **3c** formed multi-molecular assembles. However, DLS analysis could not give aggregation numbers for these assembles, and therefore, the average number of PTXL moieties per nanoparticle could not be estimated reliably. TEM imaging using RuO_4 as the staining agent showed that, when drop-casted from their aqueous solutions, **3a** and **3c** gave nanoparticles on TEM grids with sizes up to ~60 and ~90 nm respectively (Fig. 5). Because brush polymers with the backbone longer than the side chains typically would exhibit considerable aspect ratios,[17] the small aspect ratios or round morphologies of these nanoparticles also suggested their multi-molecular aggregated nanostructures on TEM grids.

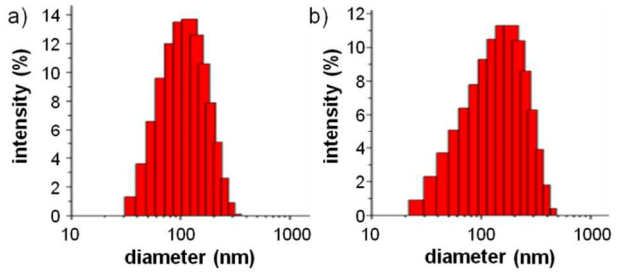

Fig. 4 DLS histograms of a) BPDC **3a**, and b) BPDC **3c** in aqueous solutions

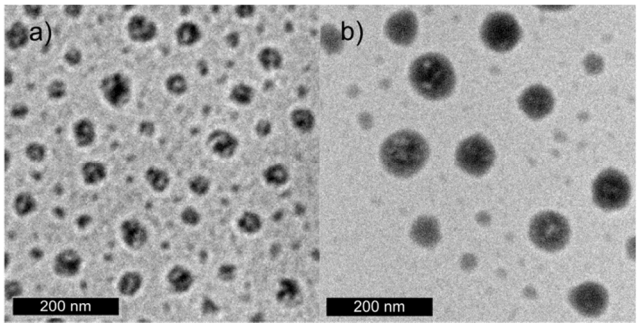

Fig. 5 TEM images of a) **3a** and b) **3c** drop-casted from aqueous solutions. Samples were stained by RuO_4.

Using **3a** as the representative sample, the release of the PTXL moieties from the diblock BPDCs by the cleavage of the cycloacetal-based conjugation linkages in phosphate buffer solutions with different pH (7.4 and 5.5) was investigated (Fig. 6). During the cleavage process, 2'-malyl PTXL, a prodrug of PTXL with the anticancer activity similar to PTXL, would be formed at first, and then transform spontaneously into PTXL (Fig. S1).[43] Our previous study of the statistical BPDC **4**, which has the same composition as **3a**, showed that the drug release was triggered in acidic conditions due to the acid-sensitive cycloacetal linkages, and 90% of the initially conjugated PTXL moieties in **4** were released within 6 h at a buffer solution with pH of 5.5.[32] However, the drug release from the diblock BPDC **3a** exhibited a lower acid-sensitivity and slower release at acidic conditions than that from the statistical BPDC **4**. As shown in Fig. 6, although the drug release at pH of 5.5 (28% at 24 h) was faster than that at pH of 7.4 (18% at 24 h) at the initial stage, the overall drug release profiles under the two pH conditions were quite similar. It took 240 h for the release of ~90% of the initially conjugated PTXL moieties on diblock BPDC **3a** in both cases. Such results may be ascribed to a slow cleavage of conjugation linkage of BPDC **3a** and a slow diffusion of the cleaved PTXL moieties from the assembled matrix. Unlike the BPDC **4** with statistical distribution of the PEG side chain and the conjugated PTXL moieties along the backbone, BPDC **3a** has its conjugated PTXL moieties not so adjacent to PEG chains. Therefore, the low concentrations of hydrated protons in the highly hydrophobic PTXL-enriched nanoscopic domains in the multi-molecular assemblies of **3a** may significantly retard the cleavage of the cycloacetal-based conjugation linkages. Moreover, because the assemblies of **3a** were much bigger than the unimolecular micelles of **4**, after the cleavage of conjugation linkages the diffusion resistance of the PTXL-based moieties would be much larger within the matrix of the assemblies of **3a**, resulting in slow diffusion of these moieties. It should be noted that DLS monitoring of the incubated buffer solutions showed relatively slight decrease of the Z_{ave} values with an increase of the incubation time, suggesting the continuous presence of multi-molecular aggregates during the drug release process (Fig. S2).

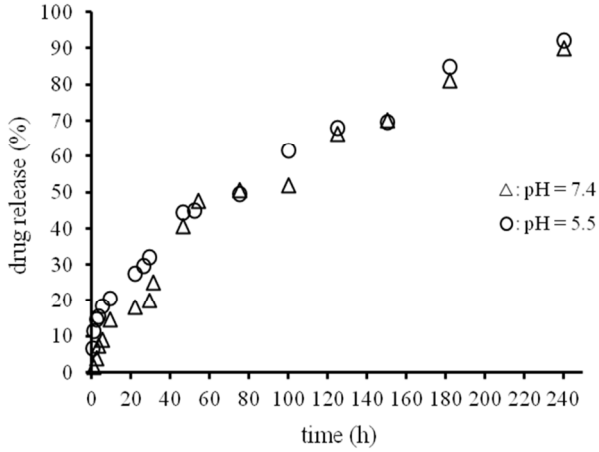

Fig. 6 Release of PTXL moieties from BPDC **3a** in pH 7.4 and pH 5.5 phosphate buffer solutions.

Selecting **3a** as the representative diblock BPDC sample, the i*n vitro* cytotoxicity of the diblock BPDCs relative to various controls was evaluated. As illustrated by the MTS assay against colon-26 cancer cells (Fig. 7), although its cytotoxic effects increased with the incubation time, the diblock BPDC **3a** (IC_{50}: considerably larger than 0.1 μg/mL for 72 h incubation) was less cytotoxic than the statistical BPDC **4** (IC_{50}: ~0.1 μg/mL for 48 h incubation) and free PTXL (IC_{50}: slightly larger than 0.1 μg/mL for 48 h incubation) at the PTXL concentrations of 0.01 and 0.1 μg/mL at the incubation times of 24, 48 and 72 h, presumably because the slow drug release from **3a** at such incubation concentrations may not result in a relatively long time period of therapeutic effective PTXL concentrations within colon-26 cells. At the PTXL incubation concentration of 1 μg/mL, **3a** exhibited similar therapeutic effects towards colon-26 cells as compared to free PTXL, but **3a** was still less effective than the statistical BPDC **4** in killing the cancer cells. In addition, the MTS assay of

the diblock BPDC **3a** against MCF-7 breast cancer cells was also performed using free PTXL and PEG-based brush polymer **5** as controls (Fig. S3). Relative to free PTXL, BPDC **3a** (IC_{50}: ~0.1 μg/mL) showed similar cytotoxicity towards MCF-7 cells in the tested PTXL incubation concentration range (0.001-1 μg/mL) at the incubation time of 48 h. Representing the PEG-based poly(**1**) block of **3a**, **5** exhibited no cytotoxic effects on these cells. Overall, the above results suggested that only the conjugated drug moieties of the BPDCs would induce cytotoxicity through drug release under the incubation conditions, and the grafting structures of BPDCs may considerably affect the cytotoxicity of BPDCs.

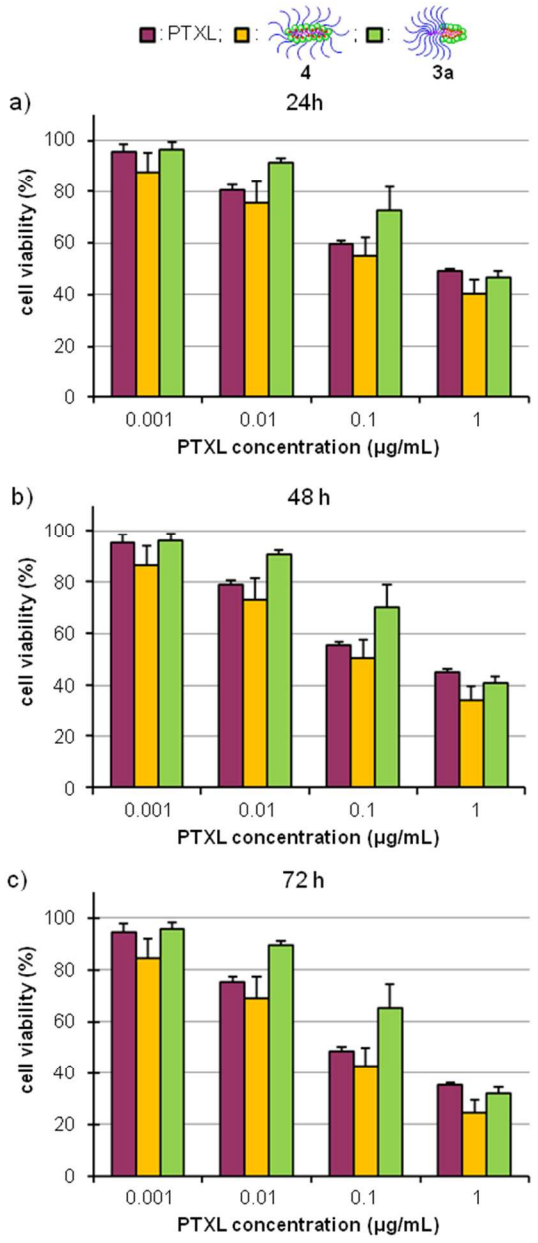

Fig. 7 Cytotoxicity of diblock BPDC **3a** against colon-26 cancer cells after 24, 48, and 72 h of incubation (free PTXL and statistical BPDC **4** as controls).

Conclusions

Well-defined PTXL-containing diblock BPDCs were successfully synthesized by sequential ROMP of a PEG-based macromonomer and a PTXL-based monomer. In principle, this "grafting-through" synthetic approach may also be applicable for the preparation of other types of block BPDCs. With a hydrophilic PEG-based block and a PTXL-based hydrophobic block, these diblock BPDCs can form multi-molecular assemblies in aqueous solutions. With the presence of cycloacetal-based cleavable conjugation linkages, the PTXL moieties in the BPDCs can be effectively released. Relative to the statistical BPDCs, these diblock BPDCs showed much lower drug release rates, presumably because of the retarded cleavage of conjugation linkages and a slow diffusion of the drug moieties within the assemblies after the cleavage. With the slow drug release behaviour, the diblock BPDCs exhibited lower cytotoxicity than their statistical analogues. The current work revealed that the distribution of grafts and drug-conjugated side groups along the backbones of BPDCs has critical influence on their assembly behaviour, drug release profile and therapeutic effects.

Acknowledgements

This work was supported by National Science Foundation (DMR-1206715) and the Mark Diamond Research Fund of the Graduate Student Association at University at Buffalo.

Notes and references

[a] *Department of Chemical and Biological Engineering, University at Buffalo, The State University of New York, Buffalo, New York 14260, USA. Email: ccheng8@buffalo.edu*

[b] *Institute for Lasers, Photonics and Biophotonics, and Department of Chemistry, University at Buffalo, the State University of New York, Buffalo, NY 14260, USA.*

† Electronic Supplementary Information (ESI) available: supporting figures. See DOI: 10.1039/b000000x/

‡ Present address: Harrens (Shandong) Testing Technology & Service Co., LTD, Shandong, China.

1 M. Elsabahy and K. L. Wooley, *Chem. Soc. Rev.*, 2012, **41**, 2545-2561.
2 R. Duncan and M. J. Vicent, *Adv. Drug Delivery Rev.*, 2013, **65**, 60-70.
3 D. Schmaljohann, *Adv. Drug Delivery Rev.*, 2006, **58**, 1655-1670.
4 E. R. Gillies and J. M. J. Fréchet, *Drug Discov. Today*, 2005, **10**, 35-43.
5 J. Kost and R. Langer, *Adv. Drug Delivery Rev.*, 2001, **46**, 125-148.
6 L. Glavas, K. Odelius and A.-C. Albertsson, *Soft Matter*, 2014, **10**, 4028-4036.
7 R. Duncan, *Nat. Rev. Cancer*, 2006, **6**, 688-701.
8 J. Kopecek, *Adv. Drug Delivery Rev.*, 2013, **65**, 49-59.
9 R. Tong and J. Cheng, *Polym. Rev.*, 2007, **47**, 345 - 381.
10 T. Nakanishi, S. Fukushima, K. Okamoto, M. Suzuki, Y. Matsumura, M. Yokoyama, T. Okano, Y. Sakurai and K. Kataoka, *J. Controlled Release*, 2001, **74**, 295-302.
11 J. Zou, F. Zhang, S. Zhang, S. F. Pollack, M. Elsabahy, J. Fan and K. L. Wooley, *Adv. Healthcare Mater.*, 2014, **3**, 441-448.
12 W. Y. Seow, J. M. Xue and Y.-Y. Yang, *Biomaterials*, 2007, **28**, 1730-1740.
13 Y. Yu, C.-K. Chen, W.-C. Law, E. Weinheimer, S. Sengupta, P. N. Prasad and C. Cheng, *Biomacromolecules*, 2014, **15**, 524-532.
14 Q. Yin, R. Tong, Y. Xu, L. W. Dobrucki, T. M. Fan and J. Cheng, *Biomacromolecules*, 2013, **14**, 920-929.
15 B. Parrish and T. Emrick, *Bioconjugate Chem.*, 2007, **18**, 263-267.
16 K. Sano, T. Nakajima, P. L. Choyke and H. Kobayashi, *ACS Nano*, 2013, 717-724.

17 S. S. Sheiko, B. S. Sumerlin and K. Matyjaszewski, *Prog. Polym. Sci.*, 2008, **33**, 759-785.

18 J. Yuan and A. H. E. Mueller, *Synthesis of Polymers*, eds.: D. A. Schlueter, C. J. Hawker and J. Sakamoto, Wiley-VCH, Weinheim, 2012, vol. 1, ch. 10, pp 263-314.

19 Z. Li, J. Ma, N.-S. Lee and K. L. Wooley, *J. Am. Chem. Soc.*, 2011, **133**, 1228-1231.

20 X. Lu, E. Watts, F. Jia, X. Tan and K. Zhang, *J. Am. Chem. Soc.*, 2014, **136**, 10214-10217.

21 J.-Z. Du, D.-P. Chen, Y.-C. Wang, C.-S. Xiao, Y.-J. Lu, J. Wang and G.-Z. Zhang, *Biomacromolecules*, 2006, **7**, 1898-1903.

22 J.-Z. Du, L.-Y. Tang, W.-J. Song, Y. Shi and J. Wang, *Biomacromolecules*, 2009, **10**, 2169-2174.

23 P. Zhao, L. Liu, X. Feng, C. Wang, X. Shuai and Y. Chen, *Macromol. Rapid Commun.*, 2012, **33**, 1351-1355.

24 C. T. Nguyen, T. H. Tran, X. Lu and R. M. Kasi, *Polym. Chem.*, 2014, **5**, 2774-2783.

25 T.-H. Tran, C. T. Nguyen, L. Gonzalez-Fajardo, D. Hargrove, D. Song, P. Deshmukh, L. Mahajan, D. Ndaya, L. Lai, R. M. Kasi and X. Lu, *Biomacromolecules*, 2014, **15**, 4363−4375.

26 Y. Q. Yang, L. S. Zheng, X. D. Guo, Y. Qian and L. J. Zhang, *Biomacromolecules*, 2011, **12**, 116-122.

27 X. Zhang, X. Zhu, F. Ke, L. Ye, E.-q. Chen, A.-y. Zhang and Z.-g. Feng, *Polymer*, 2009, **50**, 4343-4351.

28 K. Knop, D. Pretzel, A. Urbanek, T. Rudolph, D. H. Scharf, A. Schallon, M. Wagner, S. Schubert, M. Kiehntopf, A. A. Brakhage, F. H. Schacher and U. S. Schubert, *Biomacromolecules*, 2013, **14**, 2536-2548.

29 J. Zhao, S. Song, M. Zhong and C. Li, *ACS Macro Lett.*, 2012, **1**, 150-153.

30 J. A. Johnson, Y. Y. Lu, A. O. Burts, Y. Xia, A. C. Durrell, D. A. Tirrell and R. H. Grubbs, *Macromolecules*, 2010, **43**, 10326-10335.

31 J. A. Johnson, Y.-Y. Lu, A. O. Burts, Y.-H. Lim, M. G. Finn, J. T. Koberstein, N. J. Turro, D. A. Tirrell and R. H. Grubbs, *J. Am. Chem. Soc.*, 2011, **133**, 559-566.

32 J. Zou, G. Jafr, E. Themistou, Y. Yap, Z. A. P. Wintrob, P. Alexandridis, A. C. Ceacareanu and C. Cheng, *Chem. Comm.*, 2011, **47**, 4493-4495.

33 Y. Yu, J. Zou, L. Yu, W. Ji, Y. Li, W.-C. Law and C. Cheng, *Macromolecules*, 2011, **44**, 4793-4800.

34 Y. Yu, C.-K. Chen, W.-C. Law, J. Mok, J. Zou, P. N. Prasad and C. Cheng, *Molecular Pharmaceutics*, 2013, 10, 867-874.

35 Y. Yu, C.-K. Chen, W.-C. Law, H. Sun, P. N. Prasad and C. Cheng, *Polym. Chem.*, 2015, **6**, 953-961.

36 L. Liao, J. Liu, E. C. Dreaden, S. W. Morton, K. E. Shopsowitz, P. T. Hammond and J. A. Johnson, *J. Am. Chem. Soc.*, 2014, **136**, 5896-5899.

37 T. A. Willey, E. J. Bekos, R. C. Gaver, G. F. Duncan, L. K. Tay, J. H. Beijnen and R. H. Farmen, *J. Chromatogr. Biomed. Appl.*, 1993, **621**, 231-238.

38 J. S. Trent, *Macromolecules*, 1984, **17**, 2930-2931.

39 T.-L. Choi and R. H. Grubbs, *Angew. Chem. Int. Ed.*, 2003, **42**, 1743-1746.

40 Y. Xia, B. D. Olsen, J. A. Kornfield and R. H. Grubbs, *J. Am. Chem. Soc.*, 2009, **131**, 18525-18532.

41 Z. Li, J. Ma, C. Cheng, K. Zhang and K. L. Wooley, *Macromolecules*, 2010, **43**, 1182-1184.

42 Y. Li, J. Zou, B. P. Das, M. Tsianou and C. Cheng, *Macromolecules*, 2012, **45**, 4623-4629.

43 E. W. P. Damen, P. H. G. Wiegerinck, L. Braamer, D. Sperling, D. de Vos and H. W. Scheeren, *Bioorg. Med. Chem.*, 2000, **8**, 427-432.

TOC:

The synthesis, characterization and property studies of paclitaxel (PTXL)-containing brush polymer-drug conjugates (BPDCs) is presented and the influence of grafting structures of BPDCs on their assembly behaviour, drug release profile and therapeutic effects is discussed in this article.